Uncertainty analysis of conditions in the test section of the T4 shock tunnel

by

D.J. Mee

Department of Mechanical Engineering
The University of Queensland
Research Report No. 4/93
1993

Uncertainty analysis of conditions in the test section of the T4 shock tunnel

By D.J. Mee
Department of Mechanical Engineering,
The University of Queensland.

Summary

A method is presented for estimating the uncertainties in the flow conditions at the exit of the nozzle of the T4 shock tunnel in the Department of Mechanical Engineering at The University of Queensland. The method used to estimate the uncertainties is presented along with results for some test conditions. Four conditions are considered in detail - each for the Mach 5 nozzle with air as the test gas. The stagnation enthalpy for these conditions varies from 3 MJ/kg to 14 MJ/kg. The accuracy of the codes used to determine the conditions is the least well known at present. The results indicate that typical uncertainties in static pressures, temperatures and densities are around ±12% to ± 15% while uncertainties in nozzle supply temperature, flow speed and Mach number are around ± 5%.

1. Introduction

The T4 shock tunnel of the Department of Mechanical Engineering at The University of Queensland produces hypervelocity flows (around 5 km/s) of about 1 ms duration. The facility is described in Stalker and Morgan (1988). The free-stream conditions in the test section (pressure, temperature, flow speed, etc.) are usually not measured explicitly but are calculated from other measured quantities using a number of numerical codes. The codes typically used and the input parameters required are detailed below.

ESTC: The 1-D code ESTC (McIntosh, 1968) is used to determine the nozzle supply temperature of the flow given the initial shock tube filling pressure and temperature, the speed of the shock wave in the shock tube and the nozzle supply pressure behind the reflected shock at the end of the shock tube.

NENZF: The 1-D code NENZF (Lordi et al., 1966) is used to compute the flow conditions and gas composition at the exit of the nozzle given the nozzle supply temperature and pressure and the measured Pitot pressure in the test section.

STN: The 1-D code STN (Krek and Jacobs, 1993) is used when the enthalpy is too low for NENZF to give reliable answers. It replaces both STC and NENZF. The inputs required are the shock tube filling pressure and temperature, the speed of the shock wave in the shock tube, the nozzle supply pressure and either the area ratio of the nozzle (exit area / throat area) or the ratio of Pitot pressure in the test section to nozzle supply pressure.

There have been some previous studies of the accuracy with which the properties in the test section can be predicted for Stalker-tubes (Stalker and McIntosh, 1973; Stalker and Morgan, 1988). In this report the sensitivities of the conditions in the test section to each of the inputs to the codes are determined for a range of test conditions with air as the test gas and the

Mach 5 nozzle attached to the shock tube. Estimates of typical uncertainties in the inputs are presented and it is shown how these can be used to estimate the uncertainties in test conditions. Estimates of the uncertainties in the numerical codes are also considered.

2. Basic Uncertainty Analysis

The basics of uncertainty analysis are well known (eg. Kline and McClintock, 1953; Moffat, 1982; Moffat, 1988; Holman, 1966; Bendat, 1986; Baines et al., 1991) but it is worthwhile reviewing the important aspects here.

Uncertainties are usually presented in terms of a 95% confidence interval. Thus if the nominal value of some quantity is denoted as y_{nom} when the true value is y_{true} then a result containing $x\%$ uncertainty is presented as $y_{nom} \pm x\%$ and there is a 95% probability that

$$y_{nom} - x/100*y_{nom} < y_{true} < y_{nom} + x/100*y_{nom} \ .$$

Any derived parameter, F, can be expressed as a function of various fundamental quantities, $\phi_1 \ldots \phi_N$,

$$F = F(\phi_1 \ldots \phi_N)$$

There is nominally some uncertainty in each of the fundamental quantities, such that

$$\phi_i = \phi_{i_{true}} + \delta\phi_i$$

where $\phi_{i_{true}}$ is the true value and $\delta\phi_i$ is the uncertainty. The component of uncertainty in F due to the uncertainty in ϕ_i is then

$$(\delta F)_i = \left[\frac{\partial F}{\partial \phi_i}\right] \delta\phi_i \ . \qquad (1)$$

Then, providing that the individual ϕ's are *independent* and *normally distributed*, the combined uncertainty of F is

$$\delta F = \sqrt{(\delta F)_1^2 + (\delta F)_2^2 + \ldots + (\delta F)_N^2} \ .$$

It is usually more convenient to work in terms of relative uncertainties. If the relative uncertainties in the fundamental quantities are denoted as $X_{\phi_i} = \delta\phi_i/\phi_i$, the relative uncertainty in F is denoted as $X_F = \delta F/F$, and the component of uncertainty in F due to the uncertainty in ϕ_i is $(X_F)_{\phi_i}$ then

$$X_F = \sqrt{[(X_F)_{\phi_1}]^2 + [(X_F)_{\phi_2}]^2 + \ldots + [(X_F)_{\phi_N}]^2} \ . \qquad (2)$$

If a measurement is made by two independent methods each with the same uncertainty, say $(X_F)_i$, and the mean of the measurements is taken as the measured value then the overall uncertainty in the measurement will be

$$X_F = 1/\sqrt{2}\,[(X_F)_i]\,.$$

3. Uncertainty analysis for conditions in T4

The derived parameters of interest in the test section of the T4 shock tunnel include the nozzle supply temperature, T_s, static temperature, T_e, static pressure, P_e, static density, ρ_e, Mach number, M and the flow speed, u. From the information presented in the introduction and the background in section 2, the relative uncertainty in T_s can be written as

$$(X_{T_s})^2 = \left[\frac{\partial X_{T_s}}{\partial X_{P_1}}\right]^2 + \left[\frac{\partial X_{T_s}}{\partial X_{T_1}}\right]^2 + \left[\frac{\partial X_{T_s}}{\partial X_{U_{is}}}\right]^2 + \left[\frac{\partial X_{T_s}}{\partial X_{P_s}}\right]^2$$

where X_{T_s} is the relative uncertainty in T_s, X_{P_1} is the relative uncertainty in the filling pressure, P_1, X_{T_1} is the relative uncertainty in the filling temperature, T_1, $X_{U_{is}}$ is the relative uncertainty in the incident shock speed, U_{is}, and X_{P_s} is the relative uncertainty in the nozzle supply pressure, P_s.

Similar expressions can be written for the other conditions in the test section. For example, X_{P_e}, the relative uncertainty in the static pressure in the test section, P_e, can be expressed as

$$(X_{P_e})^2 = \left[\frac{\partial X_{P_e}}{\partial X_{P_1}}\right]^2 + \left[\frac{\partial X_{P_e}}{\partial X_{T_1}}\right]^2 + \left[\frac{\partial X_{P_e}}{\partial X_{U_{is}}}\right]^2 + \left[\frac{\partial X_{P_e}}{\partial X_{P_s}}\right]^2 + \left[\frac{\partial X_{P_e}}{\partial X_{Pitot}}\right]^2$$

where notation is as above and X_{Pitot} is the relative uncertainty in P_{Pitot}, the Pitot pressure measured in the test section.

4. Estimating sensitivities

The sensitivities of the derived parameters to the fundamental quantities, the $\left[\frac{\partial F}{\partial \phi_i}\right]$ term of Eq. 1, can not be determined analytically for the conditions in the T4 shock tunnel. However they can be estimated numerically for particular test conditions by a simple perturbation exercise using the codes described in section 1. The sensitivities are estimated by perturbing each fundamental quantity about its nominal value and noting the variation that this causes in each of the derived parameters of interest. The partial derivatives are then estimated using a finite difference formula.

For example, let ϕ_{i_n} be the nominal value of a fundamental quantity and let ϕ_i^- and ϕ_i^+ be negative and positive small perturbations on this quantity respectively. Let the derived

parameter be F_n when it is calculated for all fundamental quantities taking their nominal values. Let $F_{n_{i^-}}$ be the value of the derived parameter when all fundamental quantities take their nominal values except ϕ_i which takes the value ϕ_i^- and $F_{n_{i+}}$ be the derived parameter when ϕ_i takes the value ϕ_i^+. Then the finite difference estimate of the sensitivity of F to ϕ_i is given by

$$\frac{\partial X_F}{\partial X_{\phi_i}} \approx \frac{\frac{F_{n_{i+}} - F_{n_{i^-}}}{F_n}}{\frac{\phi_i^+ - \phi_i^-}{\phi_{i_n}}}.$$

5. Example test conditions

Sensitivities have been determined as outlined in section 4 for four test conditions. The test conditions are summarized in Table 1. Test conditions 1 and 2 are at a relatively low stagnation enthalpy (nominally 3MJ/kg) but at different pressure levels. For these two conditions the properties in the test section have been calculated using the code STN. Test conditions 3 and 4 are at the "moderate" stagnation enthalpies of 11 MJ/kg and 14 MJ/kg respectively. For each of these latter two test conditions the properties in the test section have been calculated using ESTC and then NENZF.

Table 1 Input conditions for test cases

Condition	1	2	3	4
Piston-Driver Reservoir (MPa)	2.2	7.1	7.1	7.1
Driver	31.5 kPa 100% Ar	77 kPa 100% Ar	77 kPa 15% Ar 85% He	77 kPa 10% Ar 90% He
Diaphragm (mm)	2	5	5	5
P_1 (kPa)	100	256	62	40
T_1 (K)	297	297	297	297
U_{iS} (m/s)	1676	1819	3348	3785
P_s (MPa)	12.3	35.9	39.0	38.2
P_{Pitot} (kPa)	171	517	591	562

The conditions in the test section for the Mach 5 nozzle, determined from the relevant codes are summarized in Table 2. In all cases the nozzle codes (NENZF and STN) have been allowed to expand the flow to match the experimentally measured ratio of $\frac{P_{Pitot}}{P_s}$.

Table 2 Calculated conditions for test cases

Condition	1	2	3	4
Code(s) used	STN	STN	ESTC NENZF	ESTC NENZF
H_0 (MJ/kg)	2.81	3.23	10.9	14.2
T_s (K)	2440	2720	6380	7540
T_e (K)	295	358	1520	1900
P_e (kPa)	3.12	10.1	15.7	15.6
ρ_e (kg/m^3)	.0370	.0980	.0353	.0270
u (m/s)	2240	2400	4090	4560
M	6.52	6.32	5.37	5.28
γ	1.40	1.39	1.32	1.32

A sensitivity analysis as described in section 4 has been performed for each of these test conditions. The results, presented in terms of relative uncertainties, are detailed in Table 3.

Table 3 Calculated sensitivities for test conditions.

Condition	1	2	3	4
$\frac{\partial X_{T_s}}{\partial X_{P_1}}$	-0.20	-0.17	-0.13	-0.10
$\frac{\partial X_{T_s}}{\partial X_{T_1}}$	0.28	0.26	0.15	0.11
$\frac{\partial X_{T_s}}{\partial X_{U_{is}}}$	1.00	0.96	1.03	0.86
$\frac{\partial X_{T_s}}{\partial X_{P_s}}$	0.20	0.19	0.17	0.15
$\frac{\partial X_{T_s}}{\partial X_{Pitot}}$	0.00	0.00	0.00	0.00
$\frac{\partial X_{T_e}}{\partial X_{P_1}}$	-0.31	-0.29	-0.18	-0.15
$\frac{\partial X_{T_e}}{\partial X_{T_1}}$	0.45	0.44	0.23	0.17
$\frac{\partial X_{T_e}}{\partial X_{U_{is}}}$	1.59	1.61	1.57	1.23

$\frac{\partial X_{T_e}}{\partial X_{P_s}}$	-0.12	-0.12	-0.09	-0.04
$\frac{\partial X_{T_e}}{\partial X_{Pitot}}$	0.44	0.44	0.33	0.32
$\frac{\partial X_{P_e}}{\partial X_{P_1}}$	-0.10	-0.09	-0.04	-0.03
$\frac{\partial X_{P_e}}{\partial X_{T_1}}$	0.15	0.12	0.06	0.03
$\frac{\partial X_{P_e}}{\partial X_{U_{is}}}$	0.52	0.47	0.49	0.25
$\frac{\partial X_{P_e}}{\partial X_{P_s}}$	-0.40	-0.41	-0.37	-0.33
$\frac{\partial X_{P_e}}{\partial X_{Pitot}}$	1.50	1.49	1.41	1.40
$\frac{\partial X_{\rho_e}}{\partial X_{P_1}}$	0.21	0.20	0.16	0.14
$\frac{\partial X_{\rho_e}}{\partial X_{T_1}}$	-0.31	-0.31	-0.18	-0.17
$\frac{\partial X_{\rho_e}}{\partial X_{U_{is}}}$	-1.10	-1.13	-1.22	-1.25
$\frac{\partial X_{\rho_e}}{\partial X_{P_s}}$	-0.28	-0.28	-0.27	-0.28
$\frac{\partial X_{\rho_e}}{\partial X_{Pitot}}$	1.05	1.06	1.08	1.09
$\frac{\partial X_u}{\partial X_{P_1}}$	-0.11	-0.10	-0.08	-0.07
$\frac{\partial X_u}{\partial X_{T_1}}$	0.17	0.15	0.09	0.09
$\frac{\partial X_u}{\partial X_{U_{is}}}$	0.55	0.57	0.60	0.62
$\frac{\partial X_u}{\partial X_{P_s}}$	0.14	0.14	0.13	0.14
$\frac{\partial X_u}{\partial X_{Pitot}}$	-0.02	-0.02	-0.04	-0.04

$\frac{\partial X_M}{\partial X_{P_1}}$	0.05	0.04	0.02	0.01
$\frac{\partial X_M}{\partial X_{T_1}}$	0.08	0.08	0.03	0.01
$\frac{\partial X_M}{\partial X_{U_{is}}}$	-0.25	-0.23	-0.21	-0.09
$\frac{\partial X_M}{\partial X_{P_s}}$	0.19	0.20	0.18	0.16
$\frac{\partial X_M}{\partial X_{Pitot}}$	-0.24	-0.26	-0.19	-0.18

The results presented in Table 3 indicate which of the input parameters it is important to measure accurately. (Note that these sensitivities need to be considered in conjunction with the levels of uncertainty in the input parameters in order to establish the parameters contributing least and most to the overall uncertainty in the derived parameters.) It is clear that most of the derived parameters have a relatively high sensitivity the shock speed (U_{is}). As described in section 6, this is a significant point because of the variation in the shock speed along the shock tube and the uncertainty which this leads to in the value used for U_{is}. For determining the nozzle supply and static temperatures, the static density, the flow speed and the Mach number, the shock speed is the most sensitive fundamental quantity. For the static pressure in the test section the most sensitive parameter is the Pitot pressure.

These results also indicate that there are only small differences in the levels of the major sensitivities over the range of conditions considered here. Thus it might be expected that reasonable estimates of uncertainties at other conditions could be made using the sensitivities in Table 3. However conditions far from those in the table should be analysed individually using the techniques outlined in this report.

6. Uncertainties in measured quantities

In order to determine the uncertainties in the conditions in the test section, the uncertainties in the fundamental measured quantities must be estimated. The purpose of this section is to make estimates of these individual uncertainties. Each fundamental parameter is treated separately below.

The shock tube filling pressure, P_1

The accuracy of this measurement depends upon

(a) The accuracy of the gauge used to measure the pressure, and

(b) The accuracy with which the operator can fill the tube to the desired level.

There are three dial gauges (each for different pressure levels) beneath the shock tube and one digital gauge on the control pannel which can be used for measuring the shock tube pressure. The dial gauges are manufactured in the USA by Solfrunt. Gauge No. 37693 has a range 0 - 200 kPag, gauge No. 01772 is a vacuum gauge with a range -100 - 0 kPag and the third gauge has a range 0 - 800 kPag. The dial gauges have a nominal reading accuracy

of ± 3% of full scale. The gauges may be read to as low as 40% of FSD which corresponds to a measurement accuracy of ± 7.5%. The digital gauges were made in the Department's instrument workshop and are based on a strain-gauged flexible tube. No measurements of the accuracy of these gauges has been made. The gauges drift with time but if a zero is taken then the reading may be accurate to within ± 5% but without a calibration this is only speculation. The operator can typically set the shock tube pressure to within 3% of the desired value. Therefore the overall accuracy of P_1 is ± 8%.

The shock tube filling temperature, T_1

The temperature of the gas in the shock tube before a shot of the tunnel is assumed to be the ambient temperature. The tube is usually filled about 10 mins before the shot so this assumption is reasonable. The ambient temperature in the laboratory varies from about 291 K to 303 K so that if the ambient temperature for each shot is not recorded the accuracy of T_1 is ± 2%.

The shock speed in the shock tube, U_{is}

The accuracy of the shock speed used in calculating the conditions in the test section depends upon

(a) the accuracy of the timing measurement,
(b) the accuracy of the measurement of distance between timing stations, and
(c) which value of the shock speed is used.

The shock speed is measured at timing stations 1 to 3 (Figure 1) using three piezo-electric pressure transducers linked in series to a charge amplifier. The output from the charge amplifier rapidly changes as the shock wave passes each measurement station. A fourth timing can be obtained from the nozzle supply pressure measurement at the end of the shock tube. The timing of the passage of the shock wave past a timing station can be determined to within ± 1% and the distance between timing stations is known to within ± 2%. The largest uncertainty in the shock speed comes from the fact that the shock wave slows down markedly as it traverses the shock tube. Some typical results for the test conditions of section 5 are presented in Table 4. The speeds determined from the measurements are shown along with the average of these. Also indicated is the difference in shock speed from the average for each measurement. At the lower enthalpy conditions the shock speed varies almost linearly along the tube but at the highest enthalpy condition here the shock slows more rapidly towards the end of the shock tube. There are a number of methods which are used to deal with this variation in shock speed. These include taking an average of either the first two speeds or all three speeds. Another is to take the speed obtained from stations 2 and 3 (Morgan and Stalker, 1988) with a justification that is based on the slug of gas that sits at the end of the tube after being processed by the shocks. It is proposed that the gas that is processed last by the shock wave passes through the nozzle and test section first and this occurs during the nozzle start-up processes, then the gas which was processed by the shock wave when it was at a speed determined from $U_{is2\text{-}3}$ passes through the test section during the test time and the gas processed by the shock wave when it was travelling at its fastest passes through after the steady or quasi-steady test time. It is noted that there is typically little difference between $U_{is2\text{-}3}$ and $U_{is_{average}}$. A third option for shock speed may be to make use of a one dimensional code such as that of Jacobs (1993). In that code the slowing of the incident shock is simulated and it may be feasible to use the computed time variation of the supply conditions for further calculation of conditions at the times of interest.

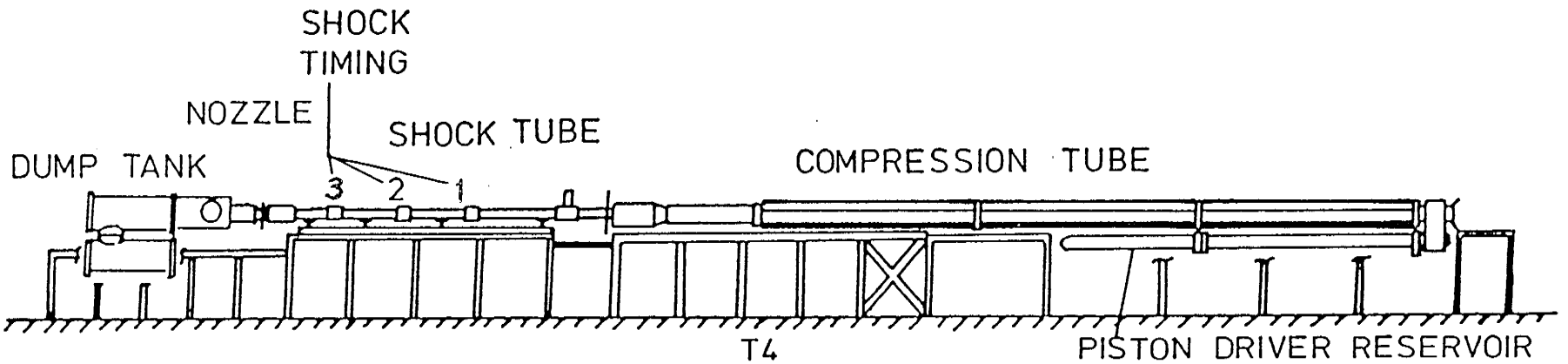

Figure 1 Timing stations for measurement of the shock speed in the shock tube.

Taking the above into consideration it is proposed that the uncertainty in shock speed during the test time will be ± 5% if either $U_{is2\text{-}3}$ or $U_{is_{average}}$ is used for further calculations. Therefore the uncertainties in measurement of shock timings and distance between measurement locations do not contribute significantly to the overall uncerainty in U_{is} which is ± 5%.

Table 4 Typical experimental shock speeds for test conditions

Condition	$U_{is1\text{-}2}$ (m/s)	$U_{is2\text{-}3}$ (m/s)	$U_{is3\text{-}P_s}$ (m/s)	$U_{is_{average}}$ (m/s)
1	1790 (+6%)	1680 (-1%)	1580 (-6%)	1690
2	1920 (+5%)	1820 (0%)	1710 (-6%)	1820
3	3570 (+7%)	3360 (+1%)	3100 (-7%)	3340
4	4070 (+7%)	3850 (+2%)	3440 (-9%)	3790

The nozzle supply pressure, P_s

The nozzle supply pressure is obtained from two piezoelectric pressure transducers (PCB Piezotronics, type 118A) which are located in the shock tube wall, on opposite sides of the tube, 65 mm upstream of the end of the shock tube. The factors affecting the accuracy of the nozzle supply pressure measurement include

(a) the accuracy of the calibration of the pressure transducer,
(b) using an average of two measurements, and
(c) the sensitivity of the transducer to installation effects.

The accuracy of the gauge calibration is estimated to be ± 2%. If two measurements are made of the nozzle supply pressure and it is assumed that the uncertainties in the two measurements are independent then the average of these measurements will have an uncertainty of $1/\sqrt{2}$ times the uncertainty in a single measurement, as discussed in section 2. Often the two gauges do not indicate the same pressure for a shot. It has been found that the indicated pressures from the gauges can be influenced by the mounting arrangement and the type and state of the protective coating on the transducer face. The condition of the leads and any movement of them during a shot may also affect the reading from the transducer. It is estimated that the accuracy of the measurements due to such factors is ± 7%. Taking this and the gauge calibration uncertainty into account the uncertainty in P_s will be ± 5% if the mean of the two nozzle supply pressure measurements is used in further calculations. If only one measurement is used the uncertainty will take the higher value.

The Pitot pressure, P_{Pitot}

The uncertainty in the Pitot pressure depends upon

(a) the accuracy of the transducer calibration,
(b) the influence of mounting of the transducer and angle of attack of the probe, and
(c) the variation in Pitot pressure in the test region.

The uncertainty due to calibration is estimated to be ± 2%. The influence of mounting the transducers is much smaller than for the nozzle supply pressure transducers and the probes are not very sensitive to the angle of attack over the range likely to be encountered (eg. see Gracey, 1956). The uncertainty due to these factors is estimated to be ± 2%. Based on experiments by Krek (1993) to measure the variation in Pitot pressure over the test section for the Mach 5 nozzle, see Figure 2, the best estimate that can be made of this variation is ± 8%. (This is based on the 14 data points presented and using Student's *t*-distribution to estimate a 95% confidence interval). Stalker and Morgan (1988) also present some Pitot pressure surveys for the Mach 5 nozzle and at the lower enthalpies of their experiments a similar variation is observed. Different levels of variation are found for different nozzles. (See Jacobs and Stalker, 1991, for experimentally measured Pitot pressure profiles for the Mach 4 and Mach 8 nozzles.) Thus the uncertainty in the Pitot pressure to be used for further calculations is dominated by the variations in Pitot pressure across the test section and for the Mach 5 nozzle this uncertainty is estimated to be ± 8%.

7. Uncertainties in derived test section quantities for test conditions

In this section the results from sections 5 and 6 are used to determine the uncertainties in the derived quantities in the test section of the T4 shock tunnel for the example test conditions. The uncertainties are calculated as outlined in section 3 and results are presented in Table 5. In this table the components of uncertainty in the derived parameters due to each of the fundamental parameters is shown as a percentage as well as the overall uncertainty in the quantities which are determined from the components as indicated in Eq. 2. In this table the notation of Eq. 2 is used.

Table 5 Components and overall uncertainties for test conditions

Condition	$(X_{T_s})_{P_1}$	$(X_{T_s})_{T_1}$	$(X_{T_s})_{U_{iS}}$	$(X_{T_s})_{P_s}$	$(X_{T_s})_{Pitot}$	X_{T_s}
1	1.6%	0.6%	5.0%	1.0%	0.0%	**5%**
2	1.4%	0.5%	4.8%	1.0%	0.0%	**5%**
3	1.0%	0.3%	5.2%	0.9%	0.0%	**5%**
4	0.8%	0.2%	4.3%	0.8%	0.0%	**4%**
	$(X_{T_e})_{P_1}$	$(X_{T_e})_{T_1}$	$(X_{T_e})_{U_{iS}}$	$(X_{T_e})_{P_s}$	$(X_{T_e})_{Pitot}$	X_{T_e}
1	2.5%	0.9%	8.0%	0.6%	3.5%	**9%**
2	2.3%	0.9%	8.1%	0.6%	3.5%	**9%**
3	1.4%	0.5%	7.9%	0.5%	2.6%	**8%**
4	1.2%	0.3%	6.2%	0.2%	2.6%	**7%**
	$(X_{P_e})_{P_1}$	$(X_{P_e})_{T_1}$	$(X_{P_e})_{U_{iS}}$	$(X_{P_e})_{P_s}$	$(X_{P_e})_{Pitot}$	X_{P_e}
1	0.8%	0.3%	2.6%	2.0%	12.0%	**12%**
2	0.7%	0.2%	2.4%	2.1%	11.9%	**12%**
3	0.3%	0.1%	2.5%	1.9%	11.3%	**12%**
4	0.2%	0.1%	1.3%	1.7%	11.2%	**11%**

	$(X_{\rho e})_{P_1}$	$(X_{\rho e})_{T_1}$	$(X_{\rho e})_{U_{iS}}$	$(X_{\rho e})_{P_s}$	$(X_{\rho e})_{Pitot}$	$X_{\rho e}$
1	1.7%	0.6%	5.5%	1.4%	8.4%	**10%**
2	1.6%	0.6%	5.7%	1.4%	8.5%	**10%**
3	1.3%	0.4%	6.1%	1.4%	8.6%	**11%**
4	1.1%	0.3%	6.3%	1.4%	8.7%	**11%**
	$(X_u)_{P_1}$	$(X_u)_{T_1}$	$(X_u)_{U_{iS}}$	$(X_u)_{P_s}$	$(X_u)_{Pitot}$	X_u
1	0.9%	0.3%	2.8%	0.7%	0.2%	**3%**
2	0.8%	0.3%	2.9%	0.7%	0.2%	**3%**
3	0.6%	0.2%	3.0%	0.7%	0.3%	**3%**
4	0.6%	0.2%	3.1%	0.7%	0.3%	**3%**
	$(X_M)_{P_1}$	$(X_M)_{T_1}$	$(X_M)_{U_{iS}}$	$(X_M)_{P_s}$	$(X_M)_{Pitot}$	X_M
1	0.4%	0.2%	1.3%	1.0%	1.9%	**3%**
2	0.3%	0.2%	1.2%	1.0%	2.1%	**3%**
3	0.2%	0.1%	1.1%	0.9%	1.5%	**2%**
4	0.1%	0.0%	0.5%	0.8%	1.4%	**2%**

The results in Table 5 show that the major source of uncertainty in the nozzle supply temperature comes from the uncertainty in shock speed. This is also the case for the static temperature in the test section although the uncertainty in the Pitot pressure does slightly increase the overall uncertainty. The uncertainty in static pressure is mainly due to the Pitot pressure variation over the test section and the sensitivity factor of approximately 1.5 leads to quite a large uncertainty in P_e. Other factors contribute negligibly to the overall uncertainty. The density accuracy is influenced most by the uncertainty in Pitot pressure but the shock speed uncertainty also contributes. The flow speed uncertainty is influenced mostly by the accuracy of the shock speed. The accuracy of the Mach number is determined by the uncertainties in Pitot pressure and shock speed.

Overall it is apparent that the uncertainties in conditions are influenced primarily by the uncertainties in the shock speed and Pitot pressure and that the levels of uncertainty in the other parameters are of less importance. Therefore, for example, even though the uncertainty in the shock tube filling pressure is estimated to be relatively large (8%), this does not seriously affect the accuracy of the predicted quantities in the test section. Also the practice of using an average ambient temperature for the initial shock tube temperature is well justified.

It is difficult to improve the accuracy of the data which contribute most to the overall uncertainty in test section parameters (the shock speed and the Pitot pressure in the test section). The shock speed variation is a function of the tunnel operation and would be difficult to alter. One possible way to improve the measurement of Pitot pressure may be to survey the test section, obtain an average Pitot pressure and relate the average to the value of Pitot pressure at the single location at which the measurement will be made during tests. However this will not alter the physical variation in Pitot pressure that exists at different

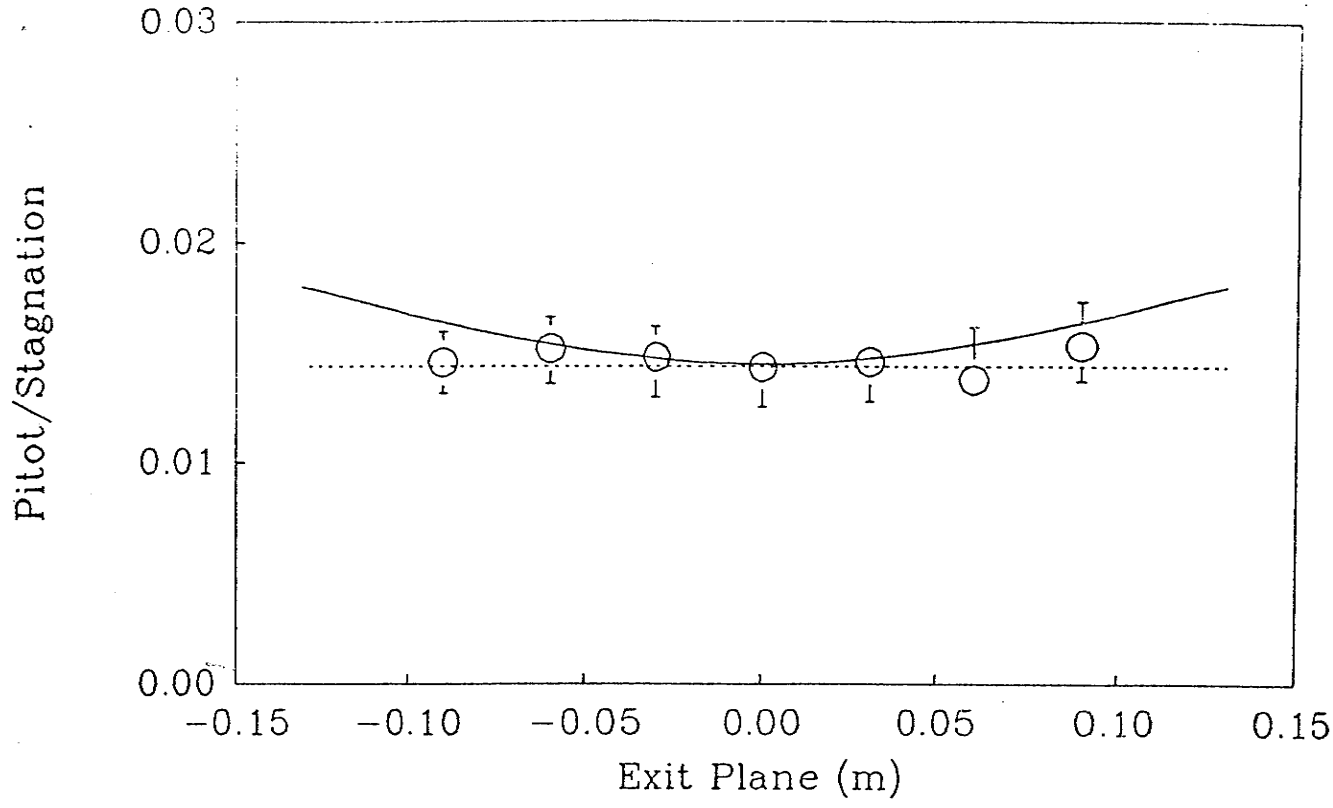

(a). Pitot pressure survey of T4 Mach 5 nozzle.
Circles - experiments, Solid line - SURF output, Dashed line - NENZF output.

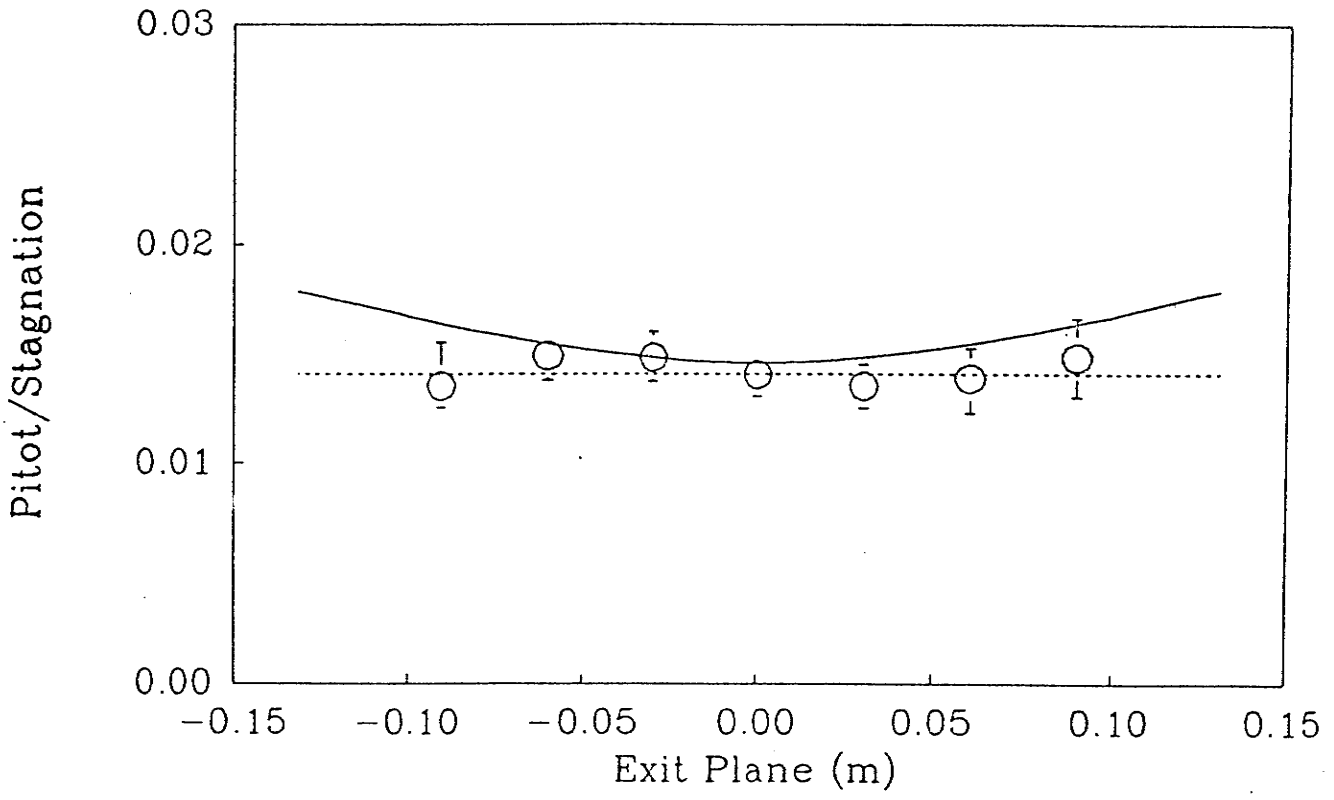

(b). Pitot pressure survey of T4 Mach 5 nozzle.
Circles - experiments, Solid line - SURF output, Dashed line - NENZF output.

Figure 2 Measured Pitot pressure surveys for T4 Mach 5 nozzle from Krek (1993). Circles - experiments; solid line - Prediction of code SURF; Dashed line - Prediction of code NENZF.

locations in the test section. If experiments are confined to a smaller portion of the test core, then it may be possible to have a reduced uncertainty on the Pitot pressure. This could be done by relating the Pitot pressure in the region of the experiments to a measurement at another location.

Bakos (1993) has collected data from a large number of shots of T4 at Test Condition 4 of the present report. He has collected the statistical parameters for these shots and results are presented in the appendix. Those data give an indication of the shot-to-shot repeatability of the conditions in the tunnel.

8. Accuracy of the numerical codes

The accuracy with which the numerical codes predict the flow conditions is difficult to assess. Some results are given in Stalker and McIntosh (1973) comparing free-stream flow speeds predicted using NENZF with those measured in a small Stalker-tube. The free-stream speed was measured with a spark-tracer technique, by observing the downstream motion of a column of the test gas which was initially heated by a spark between the tips of two electrodes in the test section. The results are presented in Figure 3 for stagnation enthalpies ranging from 5 - 40 MJ/kg. It can be seen that the measured results agree with the predictions to within about 4% over the entire range. Note however that the free-stream flow speed is not very sensitive to uncertainties in the quantities input to NENZF (Table 3).

Bakos (1993) has measured the static pressure on a flat plate placed at zero incidence near the axis of the nozzle in the test cone. As shown in Table 3, the static pressure is very sensitive to the parameters input to the numerical codes. The flat plate had eight pressure static tappings and associated transducers. Measurements were made at test condition 4 of the present report. Typical pressure traces friom these tests are shown in Figure 4. The nozzle supply, test section Pitot and plate static pressures are shown. Note that the vertical scales are different for the different pressures and that the nozzle supply pressure timescale has been delayed to account for the time-delay between the nozzle supply region and the test section. It is apparent that the static pressure decays a little more rapidly than the nozzle supply and Pitot pressures. The latter two decay at similar rates after the initial starting processes have passed. If conditions are taken at about 1 ms after flow start (where quasi-steady conditions exist according to the ratio of Pitot to nozzle supply pressures) then NENZF predicts static pressures less than 10% higher than the average of the measured values. This is within the uncertainty in static pressure for this condition determined in Table 5. However it is noted that this result is based on limited data at a single condition.

Some indication of the accuracy of the codes can be obtained by running more than one of the codes for the same input conditions and comparing the results. This has been done with ESTC and STN for the present test conditions. The results are presented in Table 6.

These results show that the nozzle supply temperatures agree to within 3%. The difference can probably be attributred to different curve fitting techniques used in determining the thermodynamic properties for each of the codes. It is more difficult to compare NENZF and STN because the latter deals only with equilibrium flows and the former will not run at low temperatures where STN is used. However, to get some indication of a comparison, NENZF was run with equilibrium chemistry and the codes were compared for the input conditions to conditions 3 & 4 of the present report. Results indicated that the major test section

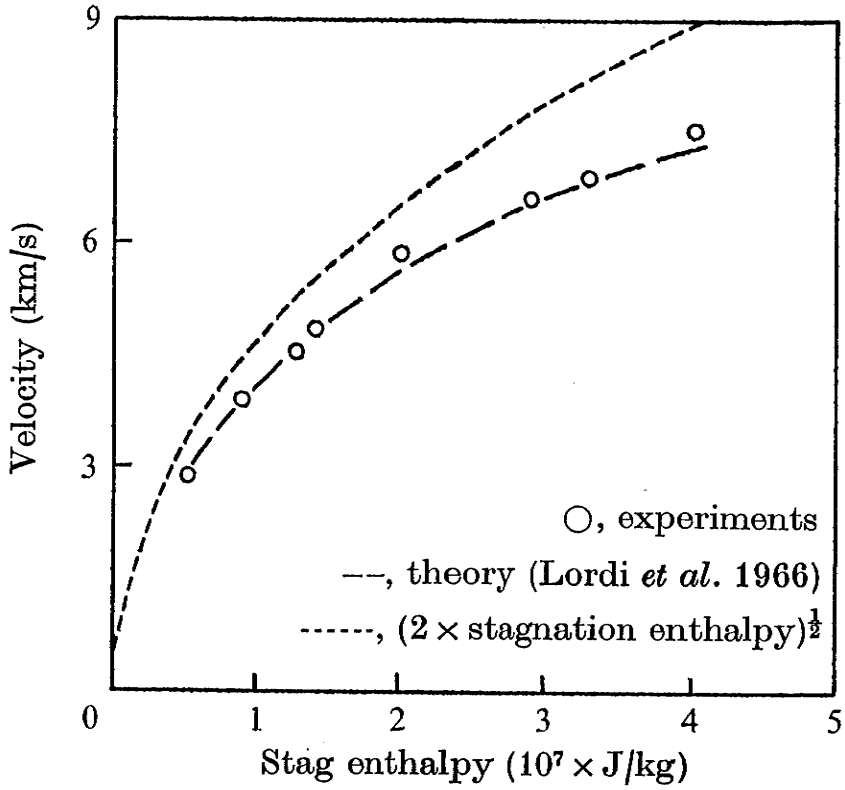

Figure 3 Measured and predicted (NENZF) flow speeds in the test section of a Stalker-tube (Stalker and McIntosh, 1973).

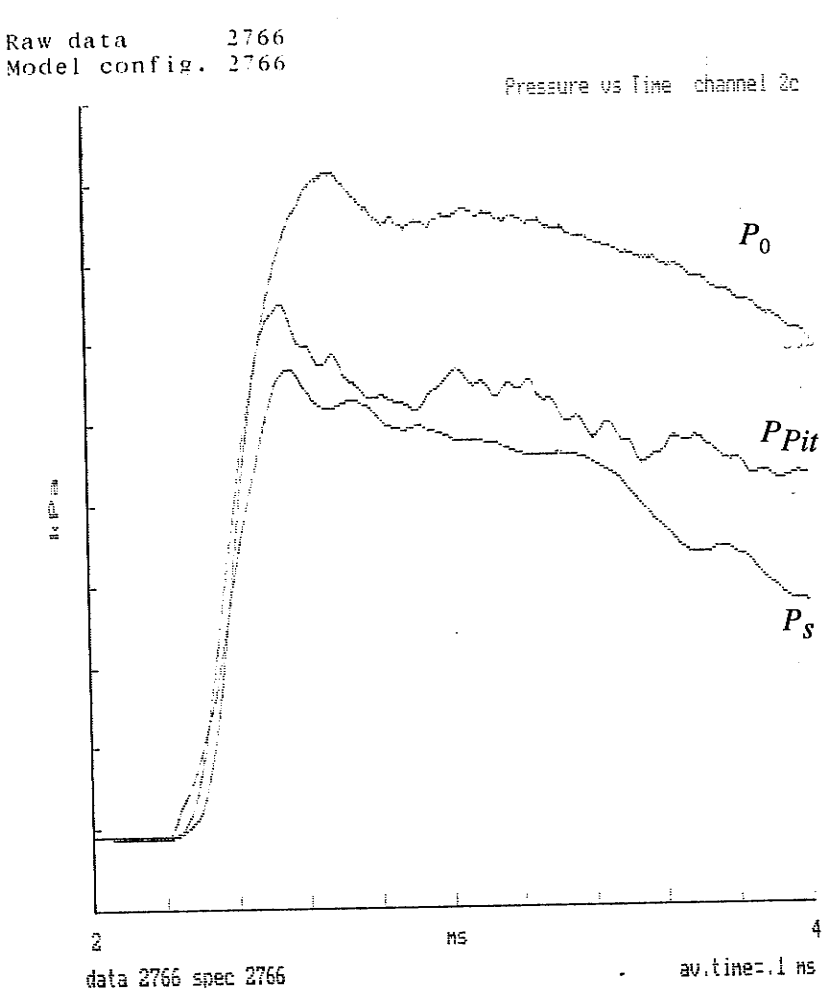

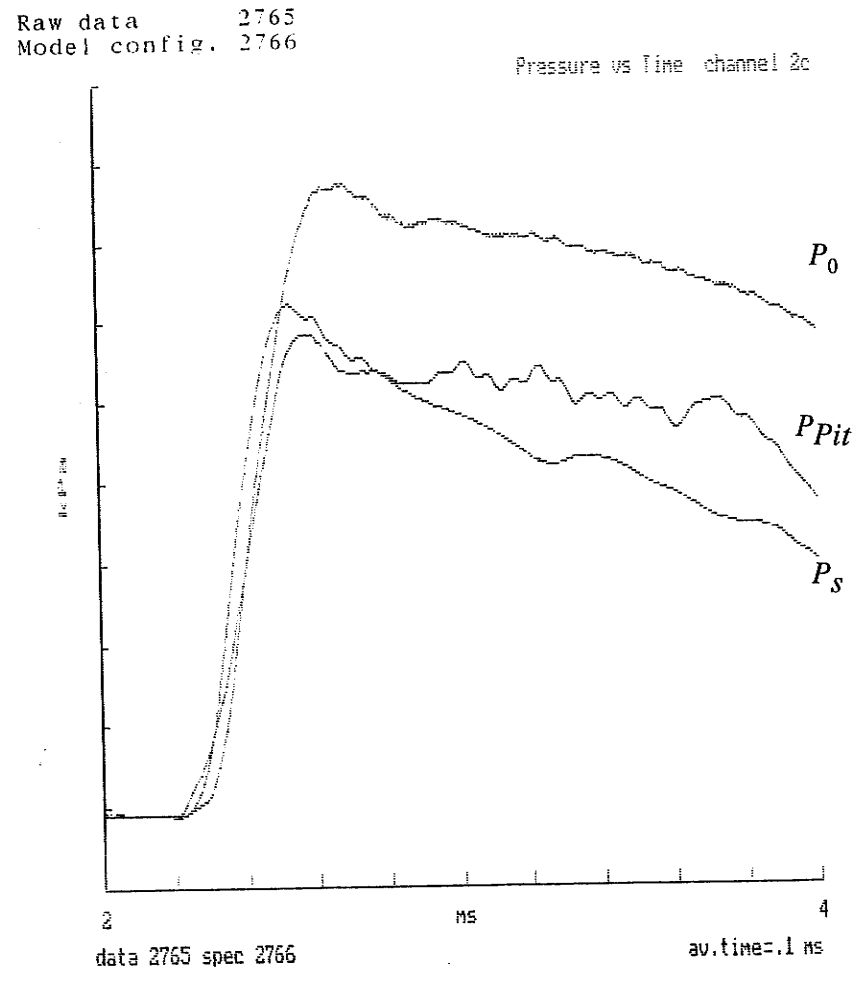

Figure 4 Pressures measured by Bakos (1993). Both tests at Condition 4. Vertical scales are different for each parameter. Static pressure at location "2c".

parameters agreed to within 10%, the largest discrepancy being in the static pressure. The following uncertainties in conditions are proposed. (These are estimates and further work is required to verify or improve the estimates.) The uncertainties in nozzle supply temperature, flow speed in the test section and flow Mach number are estimated to be ± 4%, that in static temperature and density to be ± 8% and that in the static pressure to be ± 10% .

Table 6 Comparison of ESTC and STN predictions of nozzle supply temperature

Condition	Code	P_1 kPa	T_1 K	U_{is} m/s	P_s MPa	T_s K	H_0 MJ/kg
1	ESTC	100	297	1676	12.3	2490	2.93
	STN					2440	2.81
2	ESTC	256	297	1819	35.9	2780	3.35
	STN					2720	3.23
3	ESTC	62	297	3348	39.0	6380	10.9
	STN					6210	10.5
4	ESTC	40	297	3785	38.2	7530	14.2
	STN					7440	13.8

Results are currently being analysed for tests in which the nozzle supply temperature at the end of the shock tube was measured (Wendt, 1993). Results from these tests can be used as another check on the predictions of the numerical codes.

It should be noted that if further parameters relating to the conditions in the test section are to be derived, then an analysis such as that described in Section 4 should be performed. As an example, consider the drag on a sharp cone at the four test conditions of this report (Porter, 1993). The drag can be determined theoretically by determining the contributions of the form drag due to the pressure distribution around the cone, skin friction on the cone surface and base drag. The surface pressure is determined using the method of Taylor and Maccoll (1932). The skin friction is determined assuming a laminar boundary layer and using a reference temperature (White, 1991) and for Porter's experiments the base pressure is negligible. Using the techniques of Section 4 the sensitivities of the components of the relative uncertainty in drag, X_{drag}, given in Table 7 are obtained.

Table 7 Calculated sensitivities for uncertainty in drag on a 5° cone

Condition	$\frac{\partial X_{drag}}{\partial X_{P_1}}$	$\frac{\partial X_{drag}}{\partial X_{T_1}}$	$\frac{\partial X_{drag}}{\partial X_{u_{is}}}$	$\frac{\partial X_{drag}}{\partial X_{P_s}}$	$\frac{\partial X_{drag}}{\partial X_{P_{Pitot}}}$
1	-0.09	0.13	0.44	-0.22	1.22
2	-0.07	0.10	0.37	-0.25	1.26
3	-0.05	0.07	0.50	-0.23	1.18
4	-0.05	0.06	0.44	-0.20	1.15

The contribution to overall uncertainty in the drag due to the accuracy of the numerical codes is again difficult to estimate. Since the drag is primarily a function of the quantity ρu^2 and it is estimated that the codes predict this quantity to within ± 7%, the overall uncertainty in drag is estimatd to be about ± 12% for each of the test conditions.

9. Conclusions

A technique has been presented for estimating the uncertainties in quantities calculated in the test section of the T4 Stalker tube. Four sample conditions have been analysed and estimates are presented of the uncertainties in the fundamental parameters. These combined with the sensitivities of Table 3, lead to the uncertainties presented in Table 5. The accuracies of the codes used to calculate the test section parameters are the most difficult to determine. Estimates have been made based on limited experimental data and comparisons of different codes for nominally the same conditions. Further work is required to get a better handle on the accuracy of the codes. However, combining the uncertainties in the codes with the uncertainties presented in Table 5, the following, typical uncertainties in test section parameters are obtained:

Nozzle supply temperature	± 6%
Static temperature	± 12%
Static pressure	± 15%
Static density	± 13%
Flow speed	± 5%
Test section Mach number	± 5%

If the uncertainty in Pitot pressure could be reduced to ± 5% by methods such as those outlined in Section 7, the uncertainties in static pressure and density could be reduced to:

Static pressure	± 13%
Static density	± 11%

REFERENCES

BAINES, N.C., MEE, D.J. and OLDFIELD, M.L.G. 1991 Uncertainty analysis in turbomachine and cascade testing. *Int. J. Eng. Fluid Mech.* **4** (4), 375-401.

BAKOS, R. 1993 Private communication.

BENDAT, J.S. 1986 Random data analysis and measurement procedures. 2nd ed., McGraw-Hill, New York.

GRACEY, W. 1956 Wind-tunnel investigation of a number of total-pressure tubes at high angles of attack. Subsonic, transonic and supersonic speeds. NACA TN-3641.

JACOBS , P.A. and STALKER, R.J. 1991 Mach 4 and Mach 8 axisymmetric nozzles for a high-enthalpy shock tunnel. *Aero. J.* (Nov), 324-334.

KLINE, S.J. and MCCLINTOCK, F.A. 1953 Describing uncertainties in single-sample experiments. *Mech. Eng.* (Jan.) 3-8.

KREK, R.M. 1993 Shuttle orbiter and inclined cone flows in a free piston shock tunnel. PhD thesis, The University of Queensland. Appendix B.

KREK, R.M. and JACOBS, P.A. 1993 STN, shock tube and nozzle calculations for equilibrium air. Research Report No. 2/93, Department of Mechanical Engineering, The University of Queensland.

JACOBS, P.A. 1993 Quasi-one-dimensional modelling of free-piston shock tunnels. AIAA Paper 93-0352. (Also to appear in AIAA Journal.)

LORDI, J.A., MATES, R.E. and MOSELLE, J.R. 1966 Computer program for the numerical solution of nonequilibrium expansions of reacting gas mixtures. NASA CR-472.

MCINTOSH, M.K. 1968 Computer program for the numerical calculations of frozen and equilibrium conditions in shock tunnels. Tech. Report, Australian National University.

MCINTOSH, M.K. and STALKER, R.J. 1973 Hypersonic nozzle flow of air with high initial dissociation levels. *J. Fluid Mech.* **58**(4), 749-761.

MOFFAT, R.J. 1982 Contributions to the theory of single-sample uncertainty. *Trans. ASME J. Fluids Eng.* **104**, 250-260.

MOFFAT, R.J. 1988 Describing the uncertainties in experimental results. *Exp.Therm. Fluid Sci.* **1**, 3-17.

PORTER, L. 1993 Ph.D. thesis, The University of Queensland. (To be submitted.)

STALKER, R.J. and MORGAN, R.G. 1988 The University of Queensland free piston shock tunnel T4 - initial operation and preliminary calibration. Presented at 4th National Space Engineering Symposium, Adelaide, June 12-14, 1988.

TAYLOR, G.I. and MACCOLL, J.W. 1932 The air pressure on a cone moving at high speed. *Proc. Roy. Soc. (London), Ser.A*, **139**, 278-297.

WENDT, M. 1993 Private communication.

WHITE, F.M. 1991 Viscous fluid flow. McGraw-Hill. New York.

Appendix - Tunnel Repeatability

Bakos (1993) has collected data from a large number of shots at nominally the same condition. The condition corresponds to condition 4 of the present report and there are 41 shots with air as the tes gas and 15 shots with nitrogen. The measured values for the shock speed (measured between stations 2 and 3), the two nozzle supply pressures and the Pitot pressure in the test section are presented in Figures A1 to A3. Also, shown in Figure A4, are the results for the ratio of Pitot pressure to one of the nozzle supply pressures. The statistics for these data are presented in Table A1.

Table A1 Statistics for Repeat shots of T4 at Condition 1

		Mean	Standard Deviation	95% Conf. Interval
Shock speed (m/s)	Air	3920	0.98%	± 1.9%
	Nitrogen	3930	0.86%	± 1.8%
Nozzle supply Pressure (MPa)	Probe *A*	36.3	3.6%	± 7.1%
	Probe *B*	39.8	3.0%	± 6.4%
Pitot Pressure (kPa)	Air	581	2.9%	± 5.7%
	Nitrogen	553	3.5%	± 7.5%
$\frac{P_{Pitot}}{P_{s_a}}$	Air	0.0148	4.3%	± 8.4%
	Nitrogen	0.0136	3.4%	± 7.3%

The statistics show that the shock speed is repeatable to within ± 2% but that there are quite large variations in the nozzle supply pressure. The plot of variations in the nozzle supply pressures for the two probes, Figure A2, suggests that the nozzle supply pressure does vary from shot to shot. The variations in Pitot pressure do not exactly follow the variations in the nozzle supply pressure - if they did the ratio of the two would remain constant. For the air shots, of which there are 41, the variance in the ratio of Pitot to nozzle supply pressure is almost equal to the sum of the variances in the in Pitot and stangantion pressures (0.0071 compared with 0.0083). This suggests that the variations in Pitot pressure and nozzle supply pressure are almost independent. This is not the case for the nitrogen tests, for which there are fewer results.

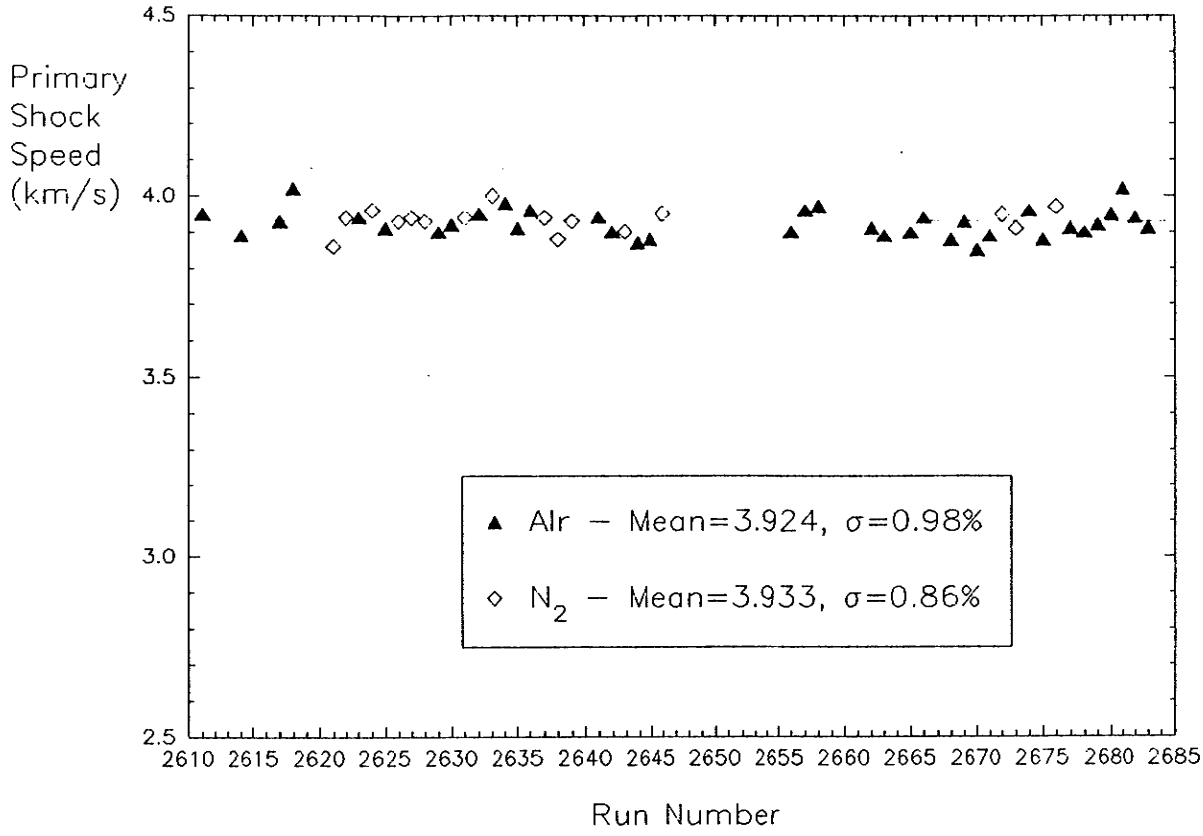

Figure A1 Shock speeds from Bakos (1993).

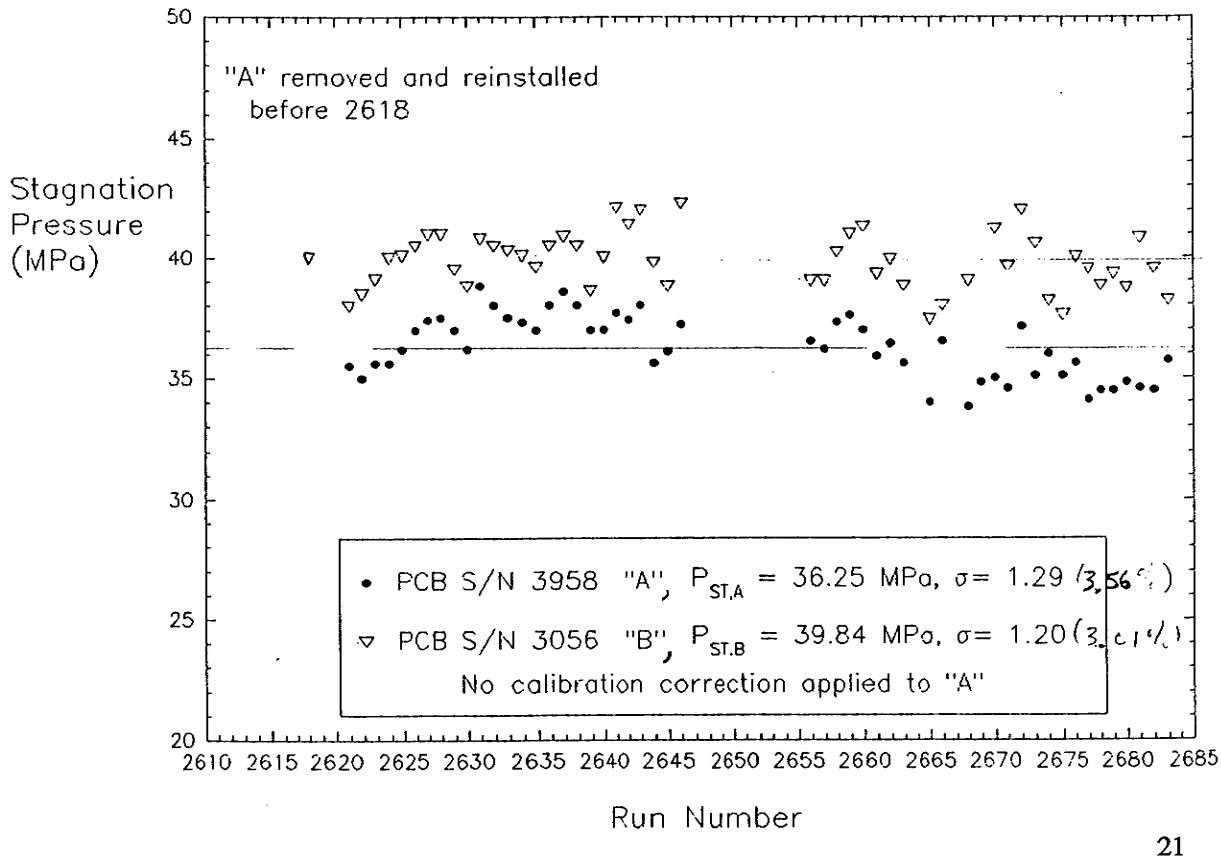

Figure A2 Stagnation pressures from Bakos (1993).

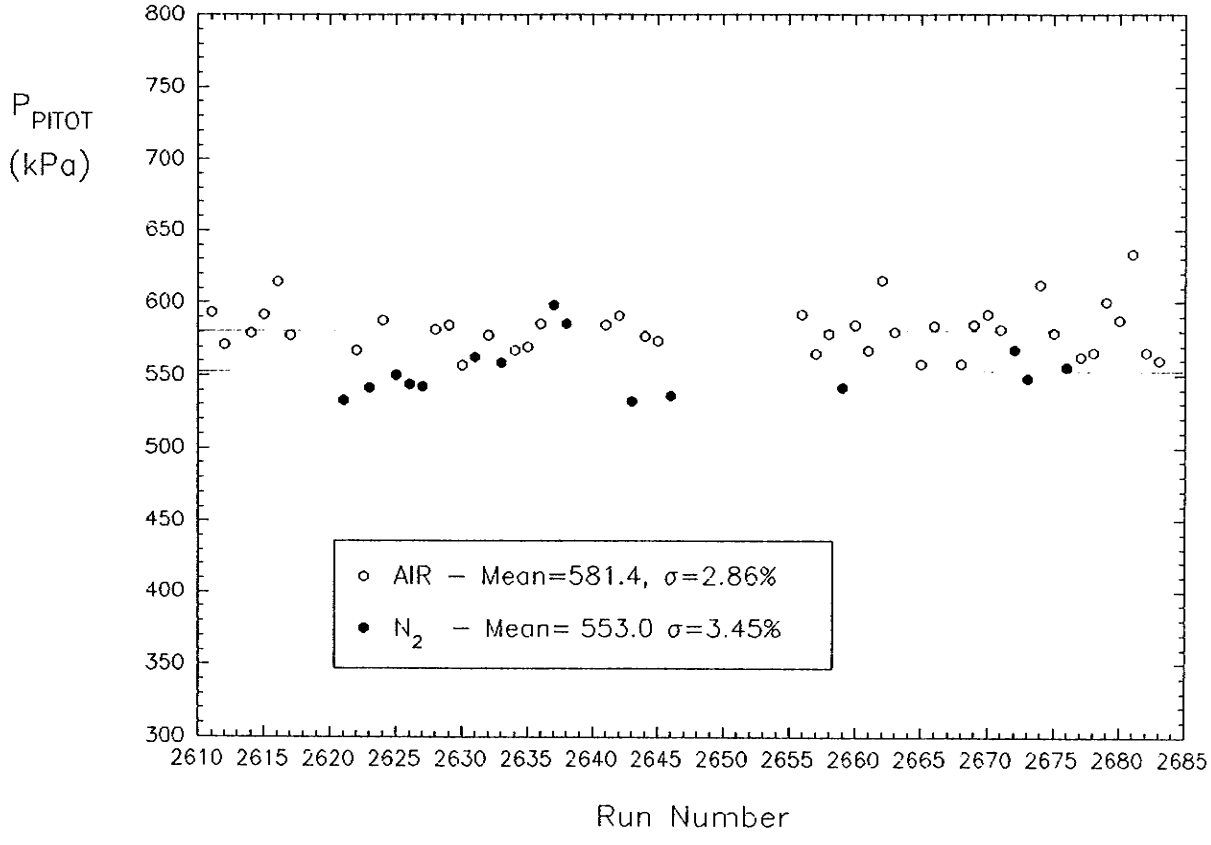

Figure A3 Pitot pressures from Bakos (1993).

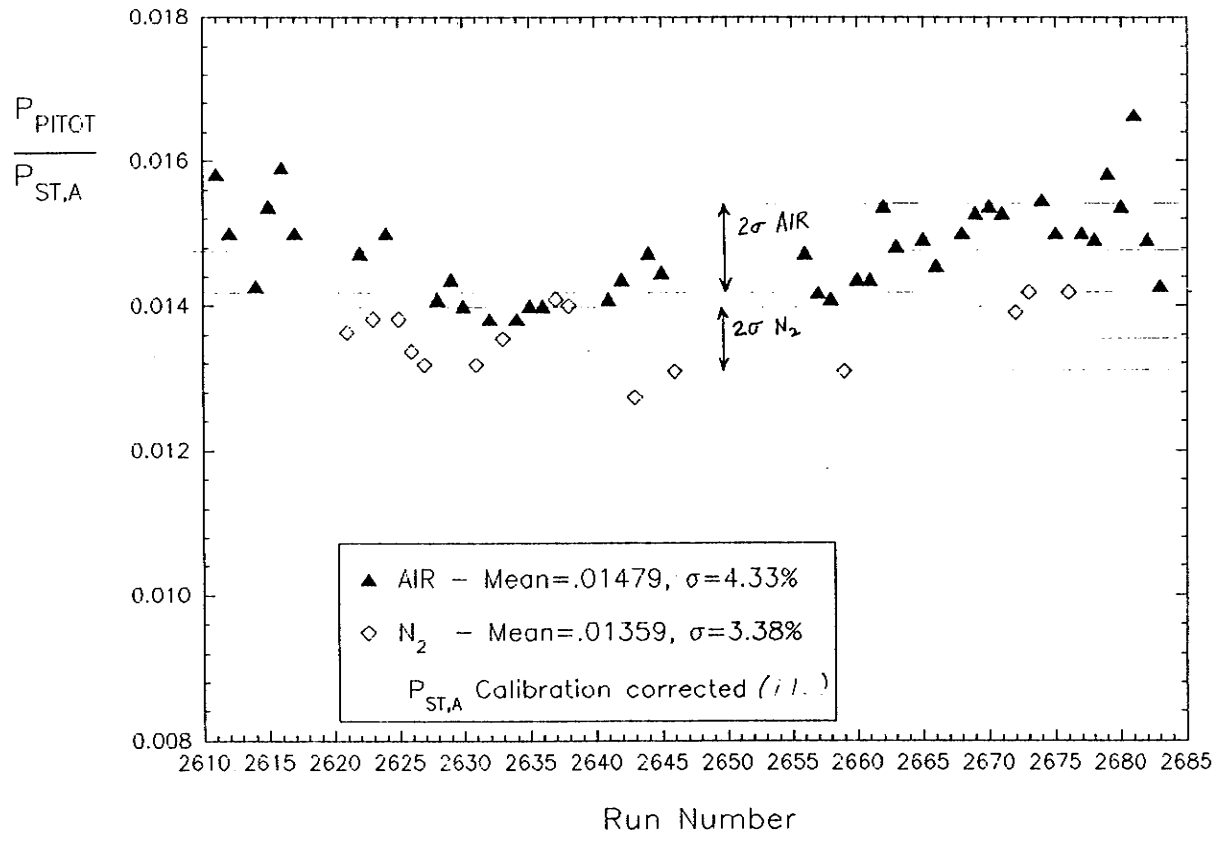

Figure A4 Ratio of Pitot to stagnation pressures from Bakos (1993).